Molecular Crystals and Liquid Crystals Science and Technology. Section A. Molecular Crystals and Liquid Crystals
Publication details, including instructions for authors and subscription information:
http://www.tandfonline.com/loi/gmcl19

# Influence of Polyimide Orientation Layer Material on the Liquid Crystal Resistivity in LCDs

N. A. J. M. Van Aerle [a]

[a] Philips Research Laboratories, Prof. Holstlaan 4, 5656AA, Eindhoven, The Netherlands

Version of record first published: 23 Sep 2006.

To cite this article: N. A. J. M. Van Aerle (1994): Influence of Polyimide Orientation Layer Material on the Liquid Crystal Resistivity in LCDs, Molecular Crystals and Liquid Crystals Science and Technology. Section A. Molecular Crystals and Liquid Crystals, 257:1, 193-208

To link to this article: http://dx.doi.org/10.1080/10587259408033776

*Mol. Cryst. Liq. Cryst.*, 1994, Vol. 257, pp. 193–208
Reprints available directly from the publisher
Photocopying permitted by license only





# Influence of Polyimide Orientation Layer Material on the Liquid Crystal Resistivity in LCDs

N. A. J. M. VAN AERLE

*Philips Research Laboratories, Prof. Holstlaan 4, 5656 AA Eindhoven, The Netherlands*

*(Received September 27, 1993; in final form January 27, 1994)*

Polyimides used as orientation layer material for liquid-crystal displays (LCDs), significantly influence the resistivity of the liquid crystal (LC) layer. The correlation between the resistivity of the polyimide and the influence of the polyimide on the LC resistivity within LCDs was investigated. Via dielectric measurements the resistivity of various polyimides was determined at elevated temperatures. The resistivity was found to be largely dependent on the polymer material used as well as on the curing temperature, and it increased with the degree of imidization. Furthermore, orientation layers of the polyimide with the lowest activation energy for ionic conduction appeared to be most capable to retain the high resistivity of the LC layer within LCD test cells. Studies on the mobility of ions in LC layers indicated that the type of ionic species diffusing from the polymer orientation layer into the LC layer also depends on the polymer used, and on the curing temperature applied. The observations can be explained by assuming that the polyimide layers contain two types of ions.

*Keywords: liquid crystal, liquid crystal display, orientation layer, polyimide, RC time, dielectric constant, loss factor, resistivity, conductivity, ionic mobility*

## 1. INTRODUCTION

Active-Matrix Liquid-Crystal Displays (AM-LCDs) are very promising flat panel displays for direct-view portable TV, projection-TV and datagraphic applications. In such AM-LCDs individual picture elements are switched by a nonlinear element (diode or transistor). In each picture element, the LC layer acts as a capacitive load to the nonlinear element which is charged during a line time of 64 μs (PAL) within the addressing cycle. The resulting voltage across the LC element must be retained for the rest of the frame time of 20 ms, before it is refreshed during the next addressing cycle. A large RC time $\tau_{RC}$ of the LC layer within each picture element is important for obtaining a good electro-optical performance of the AM-LCD.[1–3]

The RC time $\tau_{RC}$ of the LC in a display is mainly determined by the resistivity of the LC layer. It has been shown that polyimide materials used as orientation layer in LCDs can affect $\tau_{RC}$ of the LC layer significantly.[3,4] At present this effect is thought to be due to the presence of residual ionic impurities within the polyimide, which diffuse into the LC layer, thereby reducing $\tau_{RC}$.[2] Own measurements of transient currents occurring upon application of a low voltage pulse in test cells filled with nematic LC materials

showed, that the mobility of ions in the LC layer depends on the used orientation layer material. Thus the ionic species present in the LC layer depends on the orientation layer used, suggesting that various orientation layer materials contain different ionic impurities that diffuse into the LC layer.

Knowledge about the dielectric properties of the polyimide material might be helpful to understand the influence of the polyimide on the resistivity of the LC layer within LCDs. In general, ionic conduction contributes to the dielectric properties of polyimides. Ionic conduction occurs when ionizable groups, present as an impurity or as part of the polymer, dissociate to create free ions or when small amounts of water are absorbed.[5–8]

In the present article the results of a dielectric study of various polyimide materials are presented. The main goal was to investigate the correlation between the resistivity of the polyimide and the RC time of the LC layer within LCD test cells. Examples will be shown, in which the polymer as well as the degree of imidization is varied. Since the presence of a small amount of water can strongly influence the resistivity of polyimides[7,8] the water absorption/desorption behavior of the polyimides is also considered. Subsequently, the influence of the orientation layer on the resistivity of the LC layer will be discussed. Finally, some results on the mobility of ions in the LC layer of test cells containing various orientation layer materials will be described.

## 2. EXPERIMENTAL

### 2.1. Materials and LCD test cell Preparation

Three polymers were studied, which are indicated throughout this article by PI-A, PI-B and PI-C. PI-A corresponds to the fully preimidized JIB-1 polyimide, which is supplied by Japan Synthetic Rubber Co. as OPTMER™ AL-1051.[9] PI-B is an experimental polyimide of Japan Synthetic Rubber Co., which was supplied as 90% imidized material. This polymer was prepared by condensation of tetracarboxylic-acid-dianhydride, that is also used in JIB-1, and two types of diamines, viz. 4,4'-methylene-dianiline and a diamine which contains a bulky sidegroup. PI-C is the 0% imidized ZLI-2650 polymer, produced by Merck.

The polymers were spun onto ITO-coated glass substrates and cured in a vacuum oven, at the temperatures mentioned in the text. In all cases the resulting polymer layer thickness was approximately 0.1 μm. The degree of imidization of PI-C was determined by infrared absorption spectroscopy. For this determination, the infrared absorption spectrum of PI-C, heated in a vacuum oven at 300°C for several hours, was taken as reference and assumed to be 100% imidized. The degree of imidization of PI-B was also assumed to be 100% after heating for several hours at 300°C in a vacuum oven. The polymer coated substrates were rubbed with a virgin rubbing cloth for each type of polymer, and subsequently processed to test cells with a cell gap of 4 μm. The rubbing directions of both substrates were at an angle of 90°. The test cells were filled with a nematic LC mixture, supplied by Merck, containing fluorinated compounds and 0.1 wt.% of the left-handed chiral dopant ZLI-811. After filling the test cells were annealed for 2 hours at 115°C. The clearing temperature of the LC mixture was ≈ 90°C. The LC mixture was optimized for active matrix LCD applications, for which a high

voltage holding ratio is important. The bulk resistivity of the LC mixture before filling was $10^{13}\,\Omega$cm.

### 2.2. RC Time Measurements

The RC time $\tau_{RC}$ of the LC layer in test cells was determined at room temperature with a General Radio 1693 measuring bridge, operating at 25 Hz and 0.7 $V_{rms}$. In all cases two test cells, each having three measuring spots, were measured. The resulting $\tau_{RC}$-values reported in this article are the average of the six measurements.

### 2.3. Dielectric Studies

Upon application of an alternating electric field, an alternating electric polarization is produced which will lag behind the applied electric field by some phase angle. In such a case, the permittivity $\varepsilon^*$ is a complex quantity, expressed as:[10]

$$\varepsilon^* = \varepsilon' - j\varepsilon'' \tag{1}$$

where $\varepsilon'$ is the real value of the dielectric constant and $\varepsilon''$ the dielectric loss factor. Accounting for the presence of a distribution of dipole relaxation times and for ionic conductivity, $\varepsilon'$ and $\varepsilon''$ can be expressed as:

$$\varepsilon' = \varepsilon_u + (\varepsilon_r - \varepsilon_u)\frac{1}{1 + (\omega\tau_d)^{2\beta}} \tag{2}$$

$$\varepsilon'' = \frac{\sigma}{\omega\varepsilon_0} + (\varepsilon_r - \varepsilon_u)\frac{(\omega\tau_d)^{\beta}}{1 + (\omega\tau_d)^{2\beta}} \tag{3}$$

where $\tau_d$ is the mean effective dipole relaxation time, related to the time required to orient the static dipoles in the electric field. $\beta$ is a value between 0 and 1, indicating how wide the relaxation time distribution is (the lower $\beta$ the wider the distribution). For $\beta = 1$ Equations (2) and (3) change to the classic Debeye equations, derived for the presence of a single dipole relaxation time.[10,11] $\varepsilon_0$ is the permittivity of vacuum, $\varepsilon_r$ the relaxed (low frequency) permittivity, $\varepsilon_u$ the unrelaxed (high frequency) permittivity, $\omega = 2\pi\nu$ in which $\nu$ is the frequency of the applied electric field, and $\sigma$ is the bulk ionic conductivity, being the reciprocal of the resistivity $\rho$.

Dielectric measurements were performed with a Eumetric System III microdielectrometer of Micromet Instruments, in combination with low-conductivity silicon-integrated circuit sensors.[11] For excitation a sine-wave voltage with a peak-to-peak voltage of 2 V is used, giving a maximum applied electric field of 800 V/cm. At such low electrical field strength we are still measuring within the ohmic region.[12]

The sample temperature was controlled using a Mettler FP-52 hot stage. Samples were applied to the sensor from concentrated polymer solutions. The solvent was carefully evaporated by slowly heating whilst measuring the dielectric properties and sample temperature. The resulting dried samples, which were approximately 20 μm thick, were subsequently investigated.

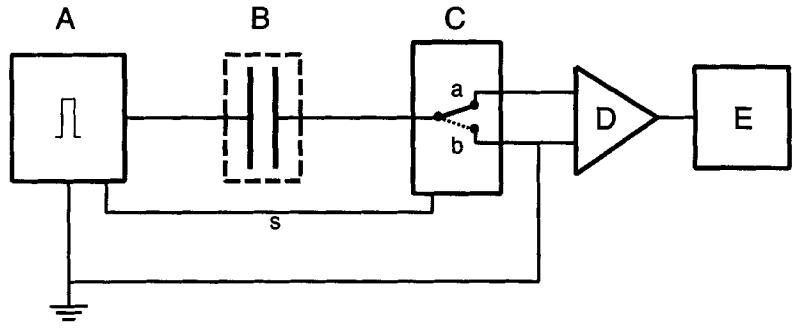


FIGURE 1 Layout of the setup used to determine transient currents in test cells filled with a liquid crystal. (A) trigger unit including an EG&G PAR-175 pulse generator; (B) test cell; (C) switch which allows the current to flow either via line (a) or via line (b); (D) Keithley 427 high speed current amplifier; (E) Philips PM-3305 memory scope which can be linked to a computer or a plotter; (s) synchronising link between the pulse generator (A) and the electric current switch (C).



### 2.4. Ionic Mobility Studies

Ionic mobilities in the LC layer of test cells were determined by transient current measurements. For this a home-built setup[13] was used, the layout of which is shown in Figure 1. When a step voltage is applied to a test cell, a fast electrode charging current and a slower and much smaller transient current can often be observed. The setup contains a switch (indicated by "C" in Figure 1), which avoids large currents to rush into the amplifier ("D" in Figure 1). This is done by allowing the initial fast electrode charging current to flow via line "b" (indicated in Figure 1) for a certain time $t_s$, after which the current is allowed to flow via line "a". This latter current is amplified and monitored. The suppression time $t_s$ can be varied manually. The minimum transient current that can be determined by the setup is approximately 0.2 nA.

In order to avoid any possible current effect from the switching of the LC layer, the measurements were performed using 1 V pulses, which are definitely below the Fredericksz threshold voltage of the LC mixture, being close to 1.8 V. A major drawback is that these low voltage pulses give weak transient currents.

The mean effective ionic mobility $\mu$ was estimated from the observed peak time $t_p$, corresponding to the peak current, using

$$\mu = \frac{d^2}{t_p V}, \tag{4}$$

where $V$ is the applied voltage and $d$ is the LC layer thickness.[14]

## 3. RESULTS AND DISCUSSION

This section is divided into five parts. First, the effect of drying of the polymers on $\varepsilon'$ and $\varepsilon''$ is discussed. Then the determination of the resistivity of the various materials at elevated temperatures is described. Subsequently, the effect of water uptake on the

polyimide resistivity is briefly discussed. This is followed by an evaluation regarding the resistivity of the polyimide and its influence on the RC time of the LC layer within test cells. Finally some results on the mobility of ions in the LC layer are discussed.

### 3.1. Effect of Drying of Polyimide on $\varepsilon'$ and $\varepsilon''$

In Figure 2 typical data are shown, measured after application of a droplet of a PI-B polymer solution to the sensor of the dielectrometer. First the temperature is increased from room temperature to 95°C to evaporate the bulk of the solvent slowly. Then the temperature is raised to 180°C to further evaporate the remaining solvent. During this procedure both $\varepsilon'$ and $\varepsilon''$ are measured for five frequencies.

The observed changes in $\varepsilon'$ (upper graph of Figure 2) and $\varepsilon''$ (lower graph of Figure 2) can be explained by evaporation of the solvent of the PI-B solution, $\gamma$-butyrolactone. $\varepsilon'$ of this solvent is 39.1 at 20°C.[15]

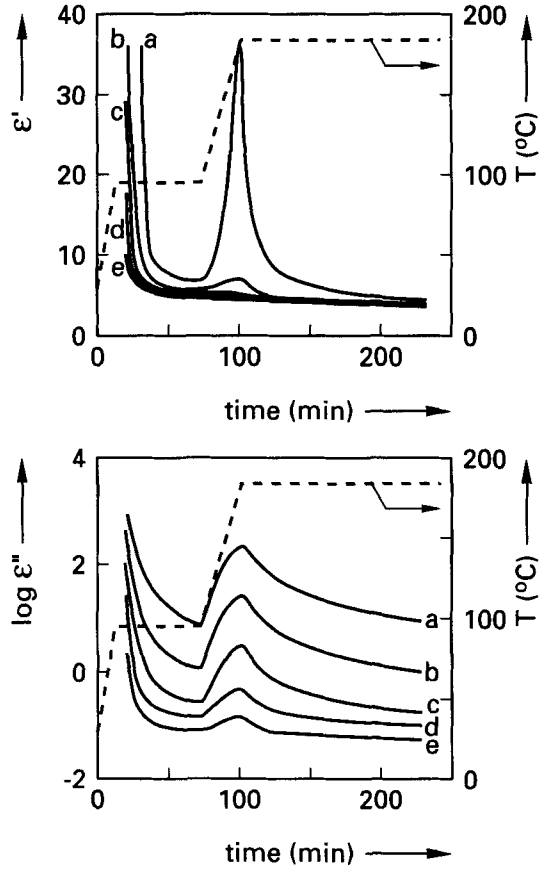


FIGURE 2 Permittivity $\varepsilon'$ (upper graph) and loss factor $\varepsilon''$ (lower graph) of PI-B polyimide as a function of time during a temperature ramp, measured at 1 Hz (**a**), 10 Hz (**b**), 100 Hz (**c**) 1 kHz (**d**) and 10 kHz (**e**). The temperature is given on the right vertical axis.

The decrease in $\varepsilon'$ can be attributed to a combination of two effects. First of all, evaporation of the high $\varepsilon'$ solvent will decrease the measured $\varepsilon'$. Additionally, solvent evaporation will lower the molecular mobility of the polymer, thus increasing the dielectric relaxation time $\tau_d$ given in Equation (2). Upon increasing the temperature from 95°C to 180°C after approximately 70 minutes, an initial strong increase of the low frequency $\varepsilon'$ is observed (see upper graph of Figure 2). This can be explained by a reduction of the relaxation time $\tau_d$ due to an increase in the molecular mobility caused by the temperature increase. However, keeping the sample at 180°C for some time, additional loss of solvent will lower $\varepsilon'$ again.

The decrease in $\varepsilon''$ (see lower graph of Figure 2) can also be attributed to the evaporation of the $\gamma$-butyrolactone. This solvent can hydrolyze in the presence of water into $\gamma$-hydroxy-butyric acid, giving rise to ionic compounds which affect the conductivity of the polymer. An equilibrium exists between the nonhydrolyzed solvent and its hydrolyzed counterpart. By evaporation of the $\gamma$-butyrolactone and water, the equilibrium shifts towards the nonhydrolyzed material. Thus, upon evaporation of $\gamma$-butyrolactone its contribution to the ionic conductivity and hence to $\varepsilon''$ will decrease and diminish to zero. Similar to $\varepsilon'$ an increase in $\varepsilon''$ is observed upon increasing the temperature from 95°C to 180°C after approximately 70 minutes, due to an initial decrease of the relaxation time $\tau_d$.

The observed changes in the dielectric properties during the drying process of PI-A and PI-C were very similar to the changes shown in Figure 2 for PI-B.

### 3.2. Resistivity of Various Polyimides

PI-A, the fully preimidized JIB-1 polyimide, is dissolved in $\gamma$-butyrolactone. After heating the sample at 300°C for more than one hour, the dielectric properties were measured as a function of frequency at various temperatures. Some results are shown in Figure 3. Figure 4 shows the results obtained for PI-B after curing the dried PI-B at 180°C for more than 2 hours. Similar measurements were performed after curing PI-B at 250°C for 3 hours, results of which are not shown here. PI-C was supplied as a 0% imidized polymer. After drying the polymer was first cured at 225°C for more than 2 hours, resulting in a degree of imidization of approximately 95%, as estimated by infrared spectroscopy. The frequency dependence of $\varepsilon'$ and $\varepsilon''$ was measured at different temperatures, and plotted in Figure 5. Finally, PI-C was heated to 290°C for more than 2 hours to increase the degree of imidization to 100%. The measured frequency dependence, not shown here, was found to be similar.

A strong increase of $\varepsilon'$ with decreasing frequency at high temperatures is observed for all three polymers studied. It is most probably caused by electrode polarization.[16]

As can be seen from Figures 3 to 5, in the low-frequency range the dielectric loss factor $\varepsilon''$ increases with temperature and decreases with frequency. Equation (3) shows that the loss factor $\varepsilon''$ contains a conductivity contribution and a dipolar contribution. For polymers the dipolar contribution rarely exceeds a value of 5. The ionic conductivity $\sigma$ can be derived from $\varepsilon''$ if the loss factor is dominated by the ionic contribution and not by the dipolar contribution. Whether $\varepsilon''$ is dominated by conduction can be determined by plotting $\log\varepsilon''$ versus $\log\nu$, as is done in Figures 3–5. If a slope of $-1$ is obtained, and $\omega\tau_d$ is less than 1 or $\varepsilon''$ exceeds a value of 5, the ionic contribution

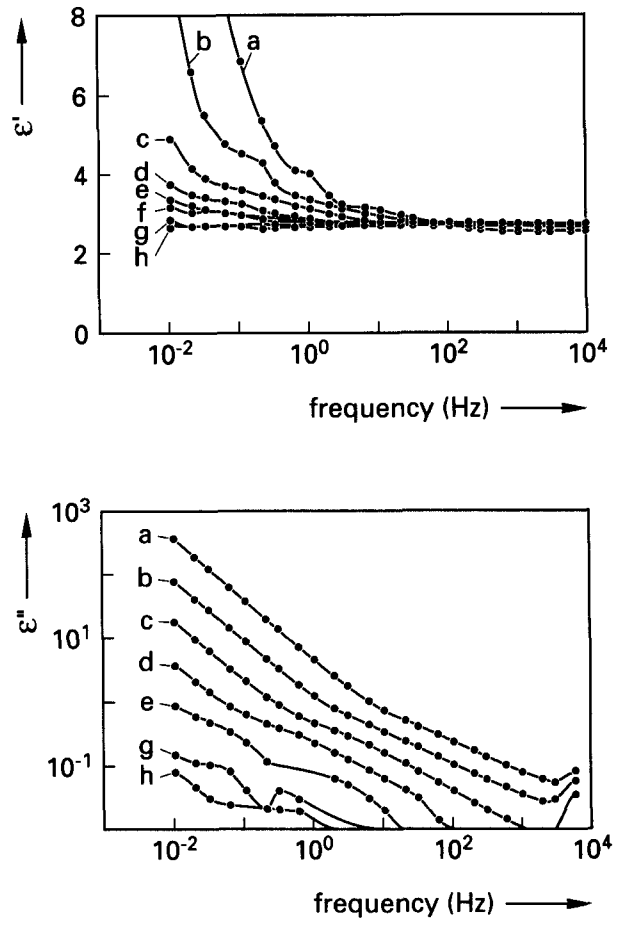


FIGURE 3 Permittivity $\varepsilon'$ and loss factor $\varepsilon''$ versus frequency for PI-A cured at 300°C, and subsequently measured at 300° (**a**), 275° (**b**), 250° (**c**), 225° (**d**), 200° (**e**), 175° (**f**), 150° (**g**), and 100°C (**h**).

dominates $\varepsilon''$. Using Equation (3), data on the curve with a slope of $-1$ can then be converted to $\sigma$ (or $\rho$) by:

$$\sigma\left(=\frac{1}{\rho}\right)=\omega\varepsilon_0\varepsilon'' \tag{5}$$

where $\omega = 2\pi\nu$, $\nu$ is the frequency of the applied electric field and $\rho$ the resistivity of the polymer. For low frequency data not falling on a curve with a slope of $-1$, Equation (5) can be used to evaluate the upper limit value of $\sigma$.

In the case of PI-A a slope of $-1$ is observed at low frequencies for temperatures exceeding 200°C (see $\log\varepsilon'' - \log\nu$ plot in Figure 3). At lower temperatures the slope deviates from $-1$, indicating that $\varepsilon''$ is no longer dominated by the ionic contribution. Here the dipolar contribution starts to affect $\varepsilon''$. Using Equation (5), $\sigma$ was calculated

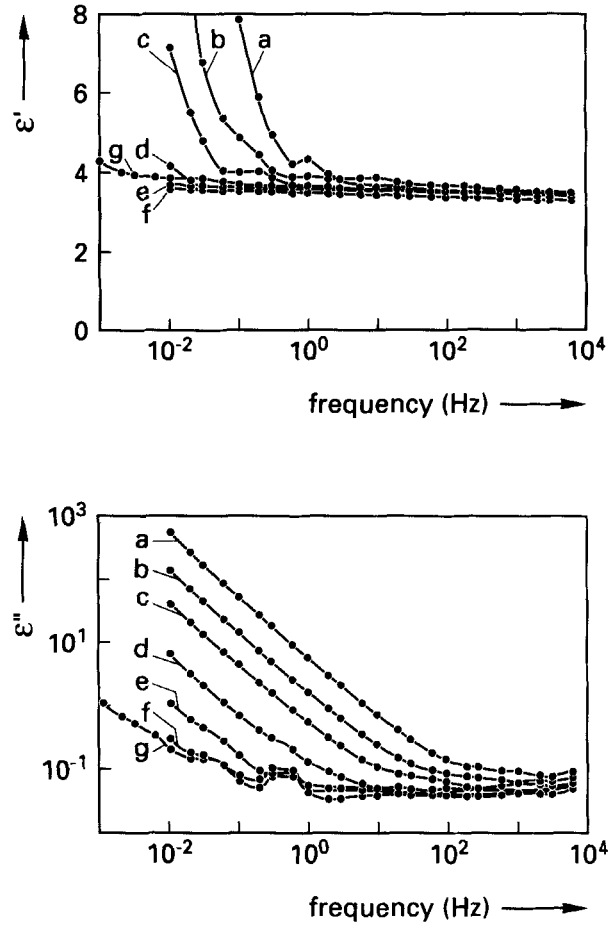


FIGURE 4 Permittivity $\varepsilon'$ and loss factor $\varepsilon''$ versus frequency for PI-B cured at 180°C, and subsequently measured at 180° (**a**), 165° (**b**), 150° (**c**), 125° (**d**), 100° (**e**), 75° (**f**), and 50°C (**g**).

for temperatures between 225 and 300°C and plotted in an Arrhenius plot (Figure 6). In the same way $\sigma$ has been evaluated for PI-B cured at 180°C and 250°C, and for PI-C cured at 225°C and 290°C. The results are also plotted in Figure 6.

The observed linear relations in the plot of $\log \sigma$ versus $1/T$ indicate that for the studied polymers the conduction process is thermally activated within the temperature region for which $\sigma$ could be evaluated. This can be expressed as:

$$\sigma = \sigma_0 \exp\left(-\frac{E_{act}}{RT}\right), \tag{6}$$

where $R$ is the gas constant, $T$ the absolute temperature, and $E_{act}$ the activation energy for the conduction process. From the slope of the curves of Figure 6 $E_{act}$ involved in the conduction process was determined. The results are given in Table I.

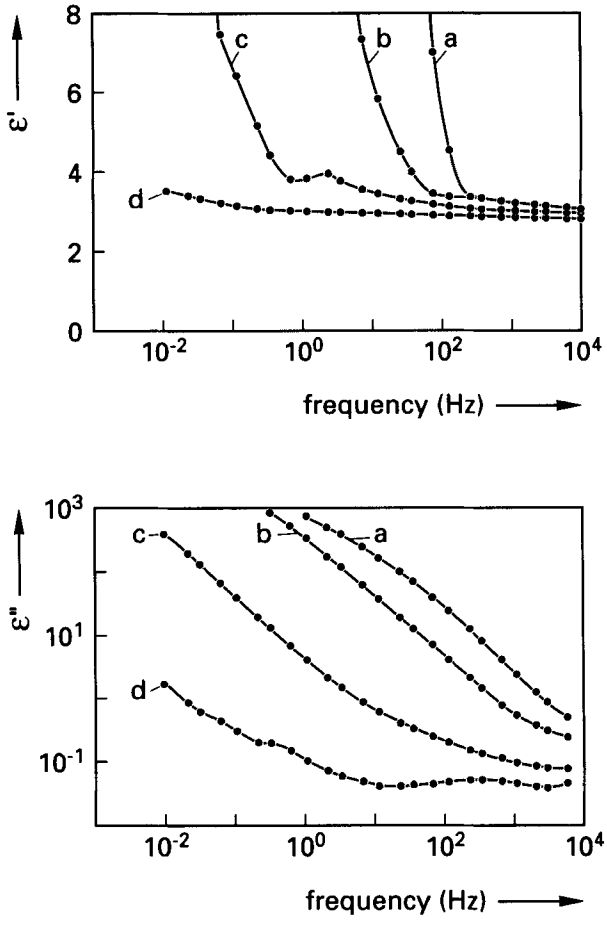


FIGURE 5 Permittivity $\varepsilon'$ and loss factor $\varepsilon''$ versus frequency for PI-C cured at 225°C, and subsequently measured at 225° (**a**), 200° (**b**), 150° (**c**), and 100°C (**d**).

As can be seen from this Table, $E_{act}$ ranges between 117 and 151 kJ/mol (i.e., between 1.22 and 1.57 eV), which agrees rather well with values given in the literature for different polyimides studied.[7,8,12,17,18] Furthermore, $E_{act}$ of PI-B and PI-C is found to be more or less independent of the curing temperature $T_{cure}$ applied. This implies that the process involved in the conduction is not affected by the degree of imidization used in our experiments. It must be noted, however, that the degree of imidization for the various samples currently measured only varied between 90 and 100%. Differences in $E_{act}$ indicate that the interaction between the ionic species and the polymer matrix differs for the various polyimides. This may be due to the presence of different ionic species in the various polyimides and/or due to differences in the chemical structure of the various polyimides. From Figure 6 it is obvious that $\sigma$ of PI-B and PI-C is significantly affected by $T_{cure}$, implying that $\sigma_0$ of Equation (6) is affected by $T_{cure}$.

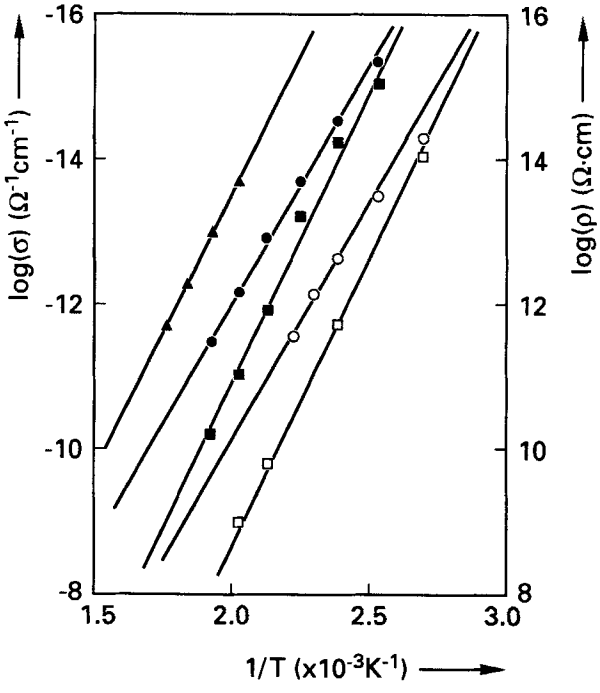


FIGURE 6 Arrhenius-plot of the conductivity $\sigma$ (left-hand-side vertical axis) versus temperature determined for PI-A (▲), PI-B cured at 180°C (○), PI-B cured at 250°C (●), PI-C cured at 225°C (□), and PI-C cured at 290°C (■). The corresponding resistivity $\rho(=1/\sigma)$ is given on the right-hand-side vertical axis.

TABLE I

Activation energy $E_{act}$ of the conduction process and the electrical resistivity $\rho_{RT}$ at room temperature, determined for various polyimides using Figure 6. $T_{cure}$ indicates the curing temperature. In addition resistivity values $\rho_{supp}$ given by the polymer suppliers are indicated

| Polyimide | $T_{cure}$ | $E_{act}$(kJ/mol) | $\log\rho_{RT}$(Ωcm) | $\log\rho_{supp}$(Ωcm) |
|---|---|---|---|---|
| PI-A | 300°C | 149 | 24 | 14.6–18(*) |
| PI-B | 180°C | 117 | 19 | 13.5 |
| PI-B | 250°C | 122 | 21 | – |
| PI-C | 225°C | 146 | 19.5 | – |
| PI-C | 290°C | 151 | 22 | 16.3 |

(*) According to the supplier the value depends on the method of determination

The polymer resistivities $\rho(=1/\sigma)$ were subsequently evaluated at room temperature by simply extrapolating the Arrhenius plots to room temperature. The resulting values are also given in Table I. The low temperature $\rho$ values obtained in this way are much higher than the values reported by the suppliers (see Table I). At least two reasons can be given for the large discrepancy. (i) The activation energy, i.e., the slope of the curves in the Arrhenius plot, may be smaller at lower temperatures.[7,8,18] Hence, extrapolation of the high temperature data to room temperature give too low $\sigma$-values and thus too

high $\rho$-values. (ii) If the temperature is decreased below 100°C, polyimides can absorb water (see next paragraph), leading to a significant increase of $\sigma$[5–8,19].

### 3.3. Water Uptake by Polyimides

As mentioned above, the resistivity of polyimides can be influenced drastically by water uptake.[5–8,19] Before considering possible effects of water uptake on the polyimide resistivity, the water absorption/desorption behavior is discussed.

Polyimide samples, kept under ambient conditions, were dried to some extent by flushing $N_2$-gas over the cured polyimide for approximately 1 hour. The used $N_2$-gas contained less than 2 volume ppm of water. Subsequently, the flushing was stopped and the sample was exposed to air with a relative humidity of 50–70%. The effect of $N_2$-flushing and subsequent exposure to air was followed by measuring $\varepsilon'$ as a function of time, at room temperature (see Figure 7 for PI-B). Upon flushing the polyimide with $N_2$ (upper graph of Figure 7) $\varepsilon'$ decreases significantly. As can be seen from the lower

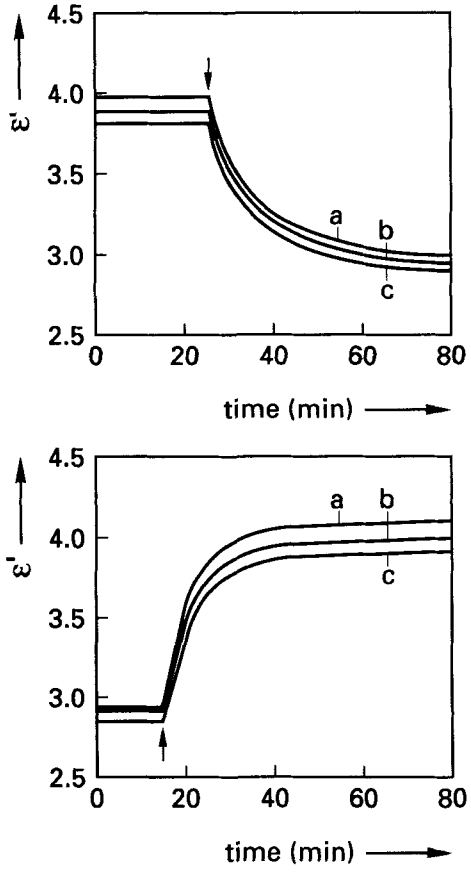


FIGURE 7 Change of permittivity $\varepsilon'$ of PI-B cured at 250°C upon flushing with $N_2$-gas (upper graph) and subsequently exposing to air (lower graph), at 1 Hz (**a**), 100 Hz (**b**), and 10 kHz (**c**). The time at which the $N_2$-flushing is started (upper graph) or stopped (lower graph), is indicated by an arrow.

graph of Figure 7, the moment the dried polyimide is exposed to air, $\varepsilon'$ increases strongly due to the absorption of water. The absorption process is more or less reversible. Assuming Fickian diffusing[20,21] a diffusion coefficient $D$ of approximately $10^{-8}$ cm$^2$/s and a water uptake of nearly 2% can be estimated for PI-B. A similar absorption/desorption behavior was observed for the other polymers studied.

The presence of water can lower $\rho$ of the polyimide layer since water partly dissociates to create ionic carriers via protolysis. It is known that at low concentrations of water the effective $\varepsilon'$ of the polymer/water system changes very little, whereas even parts per million of absorbed water can cause a substantial increase in $\sigma$ and hence a substantial decrease in $\rho$.[5,6] Therefore, at low water concentrations the dissociation of water will be the most important source of ionic carriers, leading to a decrease of $\rho$. In addition, the presence of water can increase the mobility of ionic carriers within the polymer layer, which helps to decrease $\rho$.

### 3.4. Correlation Between Polyimide Resistivity and RC Time of the LC Layer

When the RC time $\tau_{RC}$ of the LC layer is monitored as a function of storage time after filling the test cells, $\tau_{RC}$ is found to decrease gradually for several days to several weeks, before it reaches a more or less constant value. However, when the test cells are annealed for 2 hours at 115°C just after filling, $\tau_{RC}$ reaches the constant level much faster, indicating that the annealing procedure speeds up possible diffusion of ionic species from the polyimide layer into the LC. In Table II the effect of various polyimides and curing temperature $T_{cure}$ on $\tau_{RC}$ of a fluorinated LC mixture in test cells is shown, obtained after annealing the cells for 2 hours at 115°C. From this Table it is clear, that test cells with PI-B orientation layers exhibit higher $\tau_{RC}$-values than test cells with PI-A or PI-C, even when the same $T_{cure}$ is applied. Furthermore, it can be seen that $\tau_{RC}$ increases with increasing $T_{cure}$ for PI-B, but decreases with increasing $T_{cure}$ for PI-C.

TABLE II

Influence of polyimide and curing temperature $T_{cure}$ on the RC time $\tau_{RC}$ of a fluorinated liquid crystal mixture in test cells. $\tau_{RC}$ was determined after annealing the test cells for 2 hours at 115°C. In addition, the mean effective mobility $\mu$ of ions within the liquid crystal was measured at 23°C. the degree of imidization is indicated by %-imid

| Polyimide | $T_{cure}$ | %-imid | $\tau_{RC}$(sec) | $\mu$(cm$^2$/Vs) |
|---|---|---|---|---|
| PI-A | 180°C | 100% | 0.36 | $5.1 \times 10^{-6}$ |
| PI-A | 300°C | 100% | 0.32 | $8.2 \times 10^{-6}$ |
| PI-B | 180°C | 90% | 1.63 | n.d. |
| PI-B | 240°C | ≥90% | 2.30 | n.d. |
| PI-B | 300°C | 100% | 3.63 | n.d. |
| PI-C | 180°C | 72% | 0.14 | $3.5 \times 10^{-6}$ |
| PI-C | 240°C | 97% | 0.04 | $4.5 \times 10^{-6}$ |
| PI-C | 300°C | 100% | 0.03 | $5.1 \times 10^{-6}$ |

n.d.: not detectable due to the high $\tau_{RC}$

Taking the results of Figure 6 into account, it is obvious that the highest polymer resistivities are obtained for PI-A. Increasing $T_{cure}$ leads to an increase of the polymer resistivity for both PI-B and PI-C. At approximately 100°C the resistivities of PI-B cured at 250°C and PI-C cured at 290°C are comparable (see Figure 6).

At least three processes can occur upon curing at elevated temperatures,

a) increasing $T_{cure}$ of partially imidized polymer will increase the degree of imidization;
b) increasing $T_{cure}$ may expel the last remainders of solvent from the polymer;
c) increasing $T_{cure}$ may give rise to thermal decomposition.

The first two processes will lead to an increase of the resistivity, whereas the latter process can cause a decrease. That partial thermal decomposition of polymer can occur, was indicated by the fact that all three polyimides appeared to be slightly brown colored after curing at 300°C (in vacuum). When the polymers were cured at lower temperature, they appeared to be more or less colorless.

Comparing the results shown in Table II and Figure 6, no distinct correlation is observed between the absolute value of the electrical resistivity of the polyimide at high temperature and the influence of the polyimide on $\tau_{RC}$ of the LC material within test cells. For example, the highest $\tau_{RC}$ is obtained using PI-B, whereas PI-A exhibits the highest polymer resistivity. Increasing $T_{cure}$ for PI-B leads to an increase of the polymer resistivity and an increase of $\tau_{RC}$. This may be explained by an increase of the degree of imidization. PI-C, on the other hand, exhibits a decrease of $\tau_{RC}$ with increasing $T_{cure}$, whereas the polymer resistivity increases. Comparing the results of Table I and Table II shows that polyimide orientation layers exhibiting the lowest $E_{act}$ for conduction, retain $\tau_{RC}$ and hence the resistivity of the LC layer at a higher value in test cells than orientation layers exhibiting the higher $E_{act}$ for conduction.

### 3.5. Ionic Mobility Studies

The absence of a clear correlation between the resistivity of the polyimides and $\tau_{RC}$ of the LC layer strongly suggests the presence of different types of ionic species: one type of ions which affects the resistivity of the polymer, but cannot dissolve into the LC layer as free ions; and a second type of ions which affects the resistivity of the polymer and can dissolve into the LC layer as free ions, thus reducing $\tau_{RC}$ of the LC layer.

Information on the ionic species, present in the LC layer within test cells, can be obtained via transient current measurements, using the setup described in the experimental section. When a step voltage is applied to a test cell filled with a LC material, a fast electrode charging current pulse and a slower and smaller transient current with a peak can often be observed, the latter of which is generally attributed to an ionic current.[13,14,22–25] In the experiments the electrode charging current was electronically suppressed to a large extent, using the setup shown in Figure 1. To avoid additional current effects from switching of the LC layer, the measurements were performed using 1 V pulses. These pulses are definitely below the Fredricksz threshold voltage of the LC material used (which is close to 1.8 V).

Some transient currents observed for test cells with PI-C orientation layers are shown in Figure 8. As can be seen, the peak position of the transient current depends on the curing temperature of the polymer. The mean effective mobility $\mu$ of the ionic

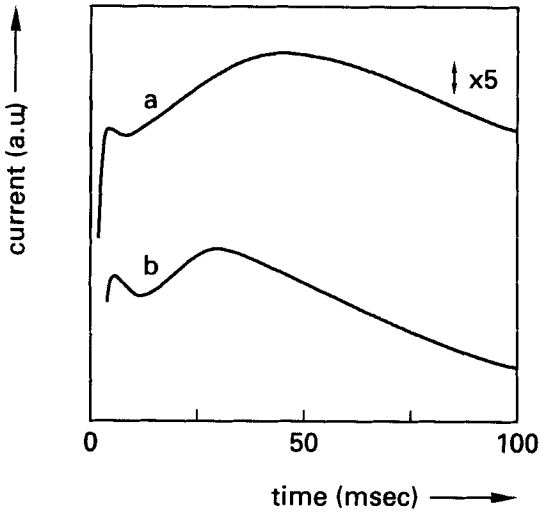


FIGURE 8 Typical traces of transient currents versus time, observed for test cells containing PI-C orientation layers cured at 180°C (**a**) and at 300°C (**b**). The LC material used is identical for both test cells. The applied voltage pulse is 1 V. The initial electrode charging peak current is electronically suppressed to a large extent. Note that the vertical scale was amplified 5 times for curve (**a**).

carriers in the LC layer is estimated from the peak position of the transient current using Equation (4). Possible variations in the thickness $d$ of the LC layer for the different test cells were corrected by using the measured capacitance of the LC layer in the test cells. This capacitance is inversely proportional to $d$ of the LC layer. The transient currents of test cells containing PI-B were too weak to determine the current peak. For PI-A and PI-C the estimated $\mu$-values are the average of two test cells. The results are given in Table II. The deviation of the estimated $\mu$-values for the two test cells is always less than $0.6 \times 10^{-6}$ cm$^2$/Vs. Hence, the differences in the $\mu$-values given in Table II are significant and beyond the error of determination.

Apparently, both the type of polymer as well as the curing temperature affect $\mu$. The observed variation in $\mu$-values indicates that the ionic impurities which reduce the resistivity of the LC layer must differ from the ionic species that are generally present in all polyimides (like $Na^+$, $K^+$ and water, which partly dissociates into $H_3^+O$ and $OH^-$). The observations suggest that the ionic species that diffuse from the orientation layer into the LC layer depend on the polymer material that is used and on the curing temperature that is applied.

Before ending this section, the question must be considered whether the ionic species detected in the LC layer are due to ionic contamination from impurities of the polymer surface or from the polymer bulk. After spin-coating the various polymers, they were all dried and cured under vacuum in the same oven. Subsequently, all layers were rubbed with a virgin rubbing cloth. Hence, polymer surface contamination that is introduced during the curing and/or rubbing process will be identical for all polymer layers studied. When the ionic species monitored by the transient current measurements arise from surface contamination, they should be identical for all test cells investigated.

However, since the observed $\mu$-values are different for the various test cells (see Table II), it can be concluded that the ionic impurities mainly arise from the polymer bulk.

## 4. CONCLUSIONS

The dielectric properties of three different polyimides used as LCD orientation layer material have been investigated to determine the correlation between the resistivity of the polyimide material and the influence of the polyimide on the RC time of the LC layer within a LCD.

Determination of the resistivity via dielectric measurements was found to be restricted to elevated temperature and low frequencies. By varying the polyimide material and its curing temperature, the resistivity of the polyimide could be influenced significantly. The resistivity increases with the degree of imidization. Furthermore, the conductivity of all the investigated polyimides was found to be thermally activated within the temperature regions studied. The corresponding activation energy ranged from 1.22 eV to 1.57 eV.

No direct correlation was found between the resistivity of the polyimide material and the effect of the polyimide on the resulting RC time of the LC layer within LCDs. However, the polymer exhibiting the lowest activation energy for ionic conduction, was found to be most capable to retain the high resistivity of the LC layer in test cells.

Ionic mobility studies show that the type of ionic species present in the LC layer within test cells depend on the polymer orientation layer material used, and on the curing temperature applied. The observations can be explained by the presence of two types of ions in the polymer layer: one type of ions, which affects the resistivity of the polymer, but cannot dissolve into the LC layer as free ions; and a second type of ions, which affects the resistivity of the polymer and can dissolve into the LC layer as free ions, thus reducing $\tau_{RC}$ of the LC layer.

Further research will be necessary to determine the actual type of ions we are dealing with, in order to better understand the influence of the polymer orientation layer on the resistivity of the LC layer.

### Acknowledgements

The author wishes to thank G. G. H. van de Spijker and F. J. Touwslager for their help during the various studies performed and described in this article. C. M. Groeneveld, G. T. Jaarsma, J. G. Kloosterboer and A. G. H. Verhulst are acknowledged for helpful and stimulating discussions.

### References

1. G. Weber, U. Finkenzeller, T. Geelhaar, H. J. Plach, B. Rieger and L. Pohl, *Liq. Cryst.*, **5**, 1381 (1989).
2. F. Moia and M. Schadt, *Proc. SID*, **32**, 361 (1991).
3. C. M. Groeneveld, *Proc. SID*, **32**, 369 (1991).
4. B. Rieger, E. Böhm and G. Weber, 18. Freiburger Arbeitstagung Flüssigkristalle, 16 (1989).
5. R. E. Barker and A. H. Sharbaugh, *J. Polym. Sci.: Part C*, **10**, 139 (1965).
6. R. E. Barker, *Pure & Appl. Chem.*, **46**, 157 (1976).

7. E. Sacher, *IEEE Trans. Electr. Insul.*, **EI-14**, 85 (1979).
8. F. W. Smith, H. J. Neuhaus, S. D. Senturia, Z. Feit, D. R. Day and T. J. Lewis, *J. Electron. Mater.*, **16**, 93 (1987).
9. Y. Yokoyama, M. Nishikawa and Y. Hosaka, *JAPAN DISPLAY' 89*, 384 (1989).
10. K. S. Cole and R. H. Cole, *J. Chem. Phys.*, **9**, 341 (1941)
11. S. D. Senturia and N. F. Sheppard, *Adv. Polym. Sci.*, **80**, 1–43 (1985).
12. G. M. Sessler, B. Hahn and D. Y. Yoon, *J. Appl. Phys.*, **60**, 318 (1986).
13. The setup was designed and built by A. G. H. Verhulst and F. J. Stommels
14. H. Mada and K. Osajima, *J. Appl. Phys.*, **60**, 3111 (1986).
15. *Beilstein* **17/5**, 4160 (1975).
16. V. Adamec and J. H. Calderwood, *IEEE Trans. Electr. Insul.*, **24**, 205 (1989).
17. A. J. Beuhler, M. J. Burgess, D. E. Fjare, J. M. Gaudette and R. T. Roginski, *Mat. Res. Soc. Symp. Proc.*, **154**, 73 (1989).
18. C. W. Reed, *Dielectric Properties of Polymers* (Ed. F. E. Karasz, Plenum Press, London, 1972), pp 343–369.
19. H. J. Neuhaus, G. B. Hershkowitz and S. D. Senturia, *Polyimides: Materials, Chemistry and Characterization* (Eds. C. Feger, M. M. Khojasteh & J. E. McGrath, Elsevier, Amsterdam, 1989), pp 527–535.
20. D. R. Ray, ibidem, pp 537–548.
21. D. D. Denton, D. R. Ray, D. F. Priore, S. D. Senturia, E. S. Anolick and D. Scheider, *J. Electr. Mat.*, **14**, 119 (1985).
22. T. Yanagisawa, H. Matsumoto and K. Yahagi, *Jpn. J. Appl. Phys.*, **16**, 45 (1977).
23. M. Yamashita and Y. Amemiya, *Jpn. J. Appl. Phys.*, **17**, 1513 (1978).
24. K. Okamoto, S. Nakajima, A. Itaya and S. Kusabayashi, *Bull. Chem. Soc. Jap.*, **56**, 3545 (1983).
25. B. Maximus, P. Vetter and H. Pauwels, *SID IDRC, SID91 Digest*, **53** (1991).